Available online at www.sciencedirect.com

SCIENCE DIRECT®

Journal of the European Ceramic Society 23 (2003) 115–122

www.elsevier.com/locate/jeurceramsoc

Preparation of high concentration ceramic inks for forming by jet-printing

R. Guo*, H. Qi, D. Guo, X. Chen, Z. Yang, Y. Chen

School of Materials Science and Engineering, Tianjin University, Tianjin 300072, China

Received 28 November 2001; received in revised form 21 March 2002; accepted 1 April 2002

Abstract

Reverse microemulsions (RMs) were applied to preparing ceramic inks for jet-printing forming. First of all, different RM systems were chosen and optimized in order to obtain high concentration ceramic inks. Triton X-100/co-emulsifier/oil/water RM system was systematically investigated. Different kinds and different amounts of co-emulsifier and oil phase were selected and mixed to form RM after intensively stirring. RM region in the quasi-ternary phase diagram of the system was determined. It was shown that Triton X-100/*n*-hexanol/cyclohexane/water RM system exhibited an excellent behavior in enhancing water-dissolving amount. The best composition for the maximum water content was given. Zirconium oxychloride solution and ammonia solution were then added to the above system respectively. After stirring intensively, two clear RMs were obtained. Then ZrO_2 ceramic inks were readily prepared by reaction after mixing the two RMs uniformly. The physicochemical properties of ZrO_2 ceramic inks, such as viscosity, surface tension, conductivity, stability etc. were determined. The particle size and morphology of ZrO_2 nanoparticles in the RM were observed by TEM. © 2002 Elsevier Science Ltd. All rights reserved.

Keywords: Emulsions; Inks; Powders-chemical preparation; Reverse microemulsions; ZrO_2

1. Introduction

Solid freeform fabrication (SFF) has become one of the new forming technologies of advanced ceramics since the 1990s. It can meet the special design ideas for composite materials and multifunctional materials. SFF includes selective laser sintering,[1–3] laminated object manufacturing,[4–6] fused deposition of ceramics,[7–9] stereolithography,[10–12] 3D-printing[13–15] and ink-jet printing,[16–18] each of which has its own advantages and potential applications.

Ink jet-printing forming is a novel method for shaping advanced ceramics, in virtue of the modern office computer system. The ceramic powder to be formed must be well suspended into a liquid, which is called a ceramic ink. The ink is printed onto a carrier through an ink jet-printer, just like printing an article on paper. The size and shape of the body can be easily controlled by the computer. The key point to realize in this forming is to prepare ceramic ink suitable for printing in both the aspects which now are still left to be solved: its own physicochemical properties and the match to the hardware of the printer. Therefore there are two basic requirements for ceramic inks. One is stability, dispersivity and homogeneity of the suspension. The other is that the physicochemical properties of the ceramic inks should meet the requirements of the commercially available printer because there are no dedicated printers available for this usage at present. There are two types of ink-jet printers: continuous and drop on demand, which have different requirements for ink as listed in Tables 1 and 2.[19,20] The preparation methods for ceramic inks include dispersion method,[21–25] sol method[26,27] and reverse microemulsion (RM) method,[28–31] each of which has its own advantages and disadvantages as mentioned in Ref. 28.

This paper focuses on the RM method, which was widely used to prepare nanoparticles of ceramic powder several years ago.[32–42] RM refers to a system composed of water/oil/emulsifier and/or co-emulsifier, which is located in a limited region of the ternary phase diagram of water/oil/emulsifier and/or co-emulsifier. In this region, water is spontaneously suspended into the continuous oil matrix in nanometer size (8–80 nm) with the help of emulsifier and/or co-emulsifier after stirring the

---

* Corresponding author.
E-mail address: rsguo@tju.edu.cn (R. Guo).

PII: S0955-2219(02)00088-2

Table 1
Ink properties for a continuous ink-printer

Conductivity (mS/m)	> 100
Viscosity (mPa·s)	1–10
Surface tension (mN/m)	25–70
Particle size	Micron meter, no agglomerate

Table 2
Ink properties for a drop on demand ink-printer

Viscosity (mPa·s) (25 °C)	1–30
Surface tension (mN/m)	35–60
pH	7–12
Particle size	Micron meter, no agglomerate

mixture intensively. Theoretically, this reverse microemulsion system is thermodynamically stable and transparent or translucent. The transparency of a real system will change a little with the suspended particle size. The water particles, also called water pools, provide reaction spaces for the formation of ceramic nanoparticles. Due to its high stability and good dispersion in nanometer sizes, this system has superiority to the other two methods with a great potential in preparing ceramic inks. According to these unique characteristics, it is worth trying this new way to prepare ceramic inks.

However, a reverse microemulsion system usually had a very low water-dissolving amount in previous reports. The authors mainly paid attention to producing well-dispersed nanoparticles using this method, rather than to its low water-dissolving amount, which is closely related to the solid content in the RM. When it is used to make a ceramic ink, the first task is to increase the water-dissolved amount so as to enhance the solid content as high as possible. Only then does the ceramic ink become practical for ink-jet printing forming. Unfortunately, there is an obstacle when the water amount increases according to the phase diagram. That is, when the water amount exceeds a certain extent, the reverse microemulsion will not exist any more and consequently transforms to another state. The way to solve this problem includes correct choice of a proper reverse microemulsion system, use of co-surfactant and optimization of preparation conditions. Another measure we can take is to use a bicontinuous structure, which is in a transition stage from the reverse microemulsion to macroemulsion. In this system, large amounts water can be dissolved. In this paper, the work on the choice of a proper reverse microemulsion system and use of co-surfactant is focused on. The authors have already conducted elementary investigations on this method.[27–29] This paper will further report the latest results.

Table 3
Composition of zirconium oxychloride reverse microemulsion

No.	Triton X-100/ wt.%	*n*-hexanol/ wt.%	Cyclohexane/ wt.%	$ZrOCl_2{\cdot}8H_2O^a$/ wt.%
1	34.4	23.0	42.6	60
2	34.4	23.0	42.6	70

[a] Total oil phase is 100% and zirconium oxychloride solution is added as a percentage of the oil phase.

Table 4
Composition of ammonia reverse microemulsion

No.	Triton X-100/ wt.%	*n*-hexanol/ wt.%	Cyclohexane/ wt.%	NH_4OH^a/ wt.%
1	34.4	23.0	42.6	80
2	34.4	23.0	42.6	70

[a] Total oil phase is 100% and ammonia solution is added as percentage of the oil phase.

2. Experiment

2.1. Determination of reverse microemulsion system

The RM was prepared at 20 °C, using Triton X-100 (iso-C_8H_{17}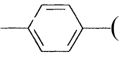$(C_2H_4)_{9.5}$H, FARCO, Chemical Supplies) as emulsifier, *n*-butanol, *n*-pentanol, *n*-hexanol (all made in China) as co-emulsifier respectively, cyclohexane, *n*-heptane, *n*-octane (all made in China) as the oil phase and deionized water. Triton X-100 and co-emulsifier were combined in the ratio of 1:0, 4:1, 3:2 and 1:1 respectively, intensively stirred for 5 min and then sealed. This mixture is referred to as S + A. The oil phase was combined with the above liquid S + A in the ratio of 5:1, 4:1, 3:1, 2:1, 1:1, 1:2, 1:3, 1:4 and 1:5, and strongly stirred for 10 min for later use. Different amounts of deionized water were added to the above mixture. They were strongly stirred again for 30 min and settled for 2 days. Then the formation of reverse microemulsion was determined through visual observation, conductivity measurement and centrifugal separation, which revealed the phase transformation or phase separation of the ternary system. Finally, the quasi-ternary phase diagrams of the systems were given and the maximum water content for each system was determined.

2.2. Preparation of ZrO_2 ceramic inks and determinations of their physicochemical properties

Different concentrations of zirconium oxychloride ($ZrOCl_2{\cdot}8H_2O$) solution and ammonia ($NH_3{\cdot}H_2O$) solution were separately prepared, and the water in the above optimized reverse microemulsion system of Triton X-100/*n*-hexane/cyclohexanol/water was replaced with an equivalent volume by these two solutions respec-

Table 5
Composition of ZrO_2 ceramic ink at 20 °C

Ink	Triton X-100/ wt.%	*n*-hexanol/ wt.%	Cyclohexane/ wt.%	Water/ wt.%	ZrO_2 Solid load/ wt.%	pH
A	22.2	14.8	27.5	33.6	1.9	9
B	24.0	16.1	29.8	28.0	2.1	6

tively, giving rise to two reverse microemulsions, whose compositions are shown in Tables 3 and 4. These two reverse microemulsions were then mixed homogeneously and the reaction of zirconium oxychloride with ammonia in the water pools happened and $Zr(OH)_4$ nanoparticles formed. The process of the reaction was controlled by the pH value through adding different amounts of the ammonia reverse microemulsion. The resulting microemulsion was referred to as ZrO_2 ceramic ink listed in Table 5. Its rheological characteristics, surface tension, conductivity, transparency and stability were determined by rheometer (WCR 300 SN 357142), surface tensiometer (self installed based on the maximum bubble pressure method), conductivity meter (DDS-11A), ultraviolet/visible spectrophotometer (750MC), respectively. The particle size in the reverse microemulsion was observed by TEM (100CX-II). Phase separation was determined by visual observation.

3. Results and discussion

3.1. Determination of the reverse microemulsion system

The quasi-ternary phase diagrams of the RM systems of Triton X-100/co-emulsifier/oil/ water with different ratios at 20 °C are shown in Fig. 1, where S + A represents the total mass of Triton X-100 and co-emulsifier, O is the mass of oil phase, and W is the mass of water. Lines a, b, c and d in each diagram represent the ratio of Triton X-100 to co-emulsifier (in mass) 1:0, 3:1, 3:2 and 1:1, respectively. The reverse microemulsion lies in the upper region of the boundary line.

It was shown from the above diagrams that the Triton X-100/co-emulsifier/oil/water reverse microemulsion systems all had a large region of the reverse microemulsion, whose area decreases with the ratio of Triton X-100 to co-emulsifier in the sequence of 3:2, 1:1, 3:1 and 1:0 for whatever combinations of co-emulsifier and oil. The maximum reverse microemulsion area, and consequently the maximum water-dissolving amount were simultaneously obtained when the ratio of Triton X-100 to co-emulsifier was 3:2. In addition, we can also see that Triton X-100/*n*-hexane/cyclohexane/water reverse microemulsion system had the maximum area of all the reverse microemulsions and the maximum water-dissolving amount (44%) resulted according to our experiments.

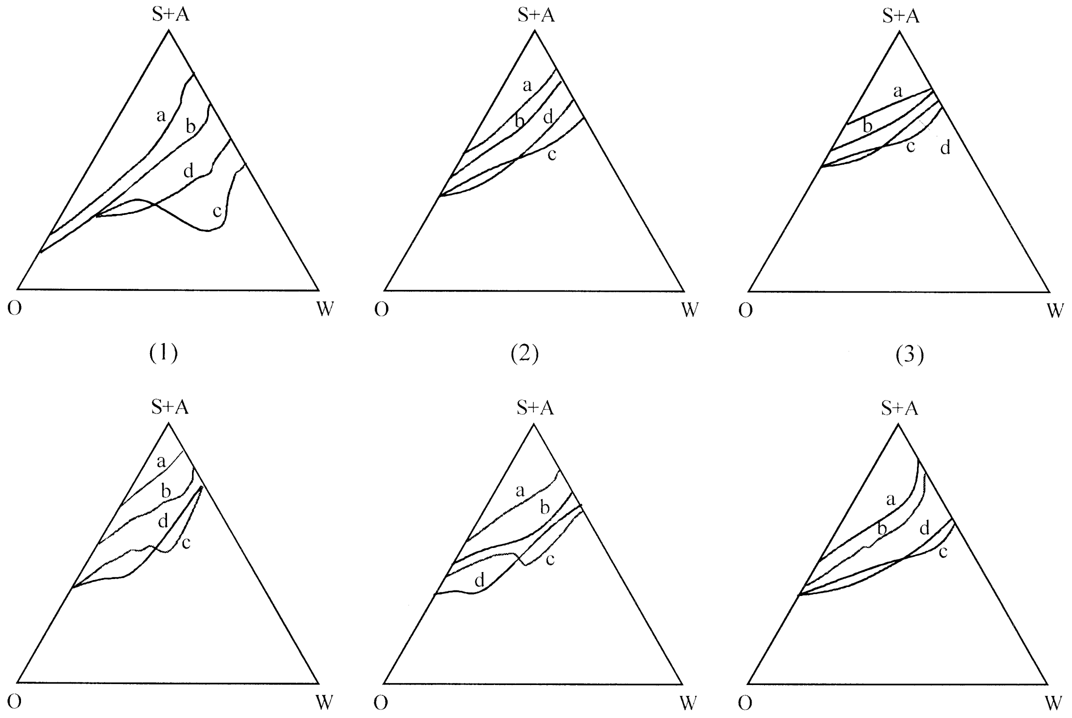

(1) (2) (3)

(4) (5) (6)

Fig. 1. Quasi-ternary phase diagrams of the reverse microemulsion systems. (1) Triton X-100/n-hexanol/cyclohexane/water; (2) Triton X-100/*n*-butanol/*n*-heptane/water; (3) Triton X-100/*n*-butanol/*n*-octane/water; (4) Triton X-100/*n*-pentanol/*n*-heptane/water (5) Triton X-100/*n*-hexanol/*n*-octane/water (6) Triton X-100/*n*-pentanol/cyclohexane/water.

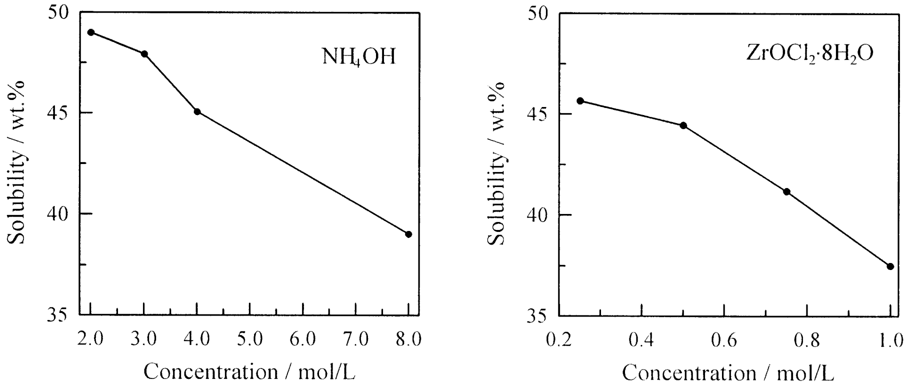

Fig. 2. Solubility limit of the reverse microemulsions.

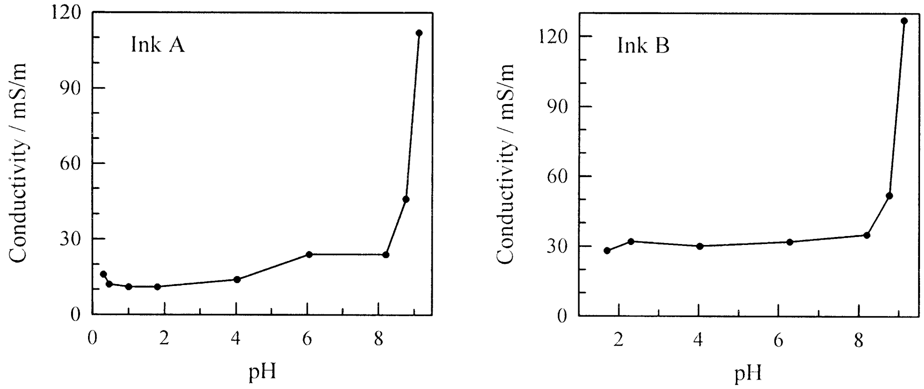

Fig. 3. The effect of pH on conductivity of the ceramic inks.

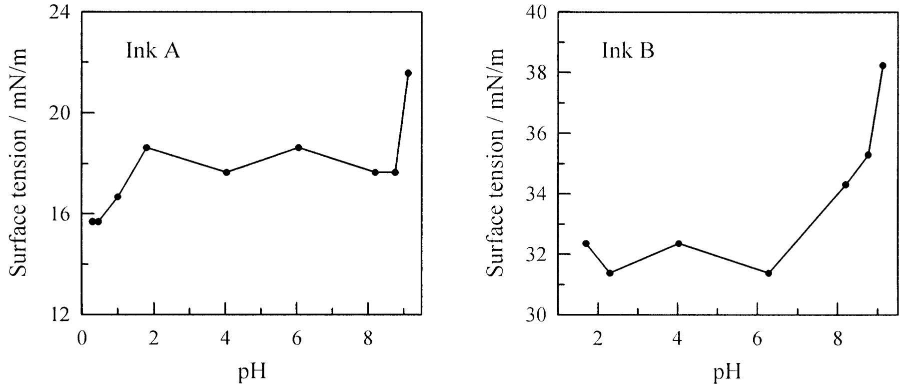

Fig. 4. The effect of pH on surface tension of the ceramic inks.

*3.2. Solubility limit of zirconium oxychloride solution and ammonia solution in the system of Triton X-100/*n*-hexane/cyclohexanol at 20 °C*

The effect of different concentrations of zirconium oxychloride solution and ammonia solution on the solubility limit in the system of Triton X-100/*n*-hexane/cyclohexanol at 20 °C was shown in Fig. 2. It can be seen from the figure that a large amount of zirconium oxychloride solution and ammonia solution can be dissolved into the system, with the maximums 46 and 49%, respectively, which was equivalent to or larger than that of the pure water. However, water content decreased with increasing the concentration for both the solutions, and the solubility drop was more severe for zirconium oxychloride solution due to the existence of

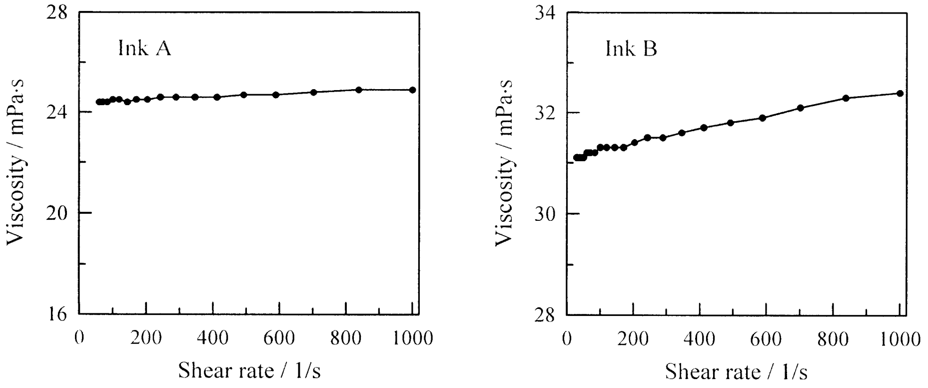

Fig. 5. The rheological characteristics of the ceramic inks.

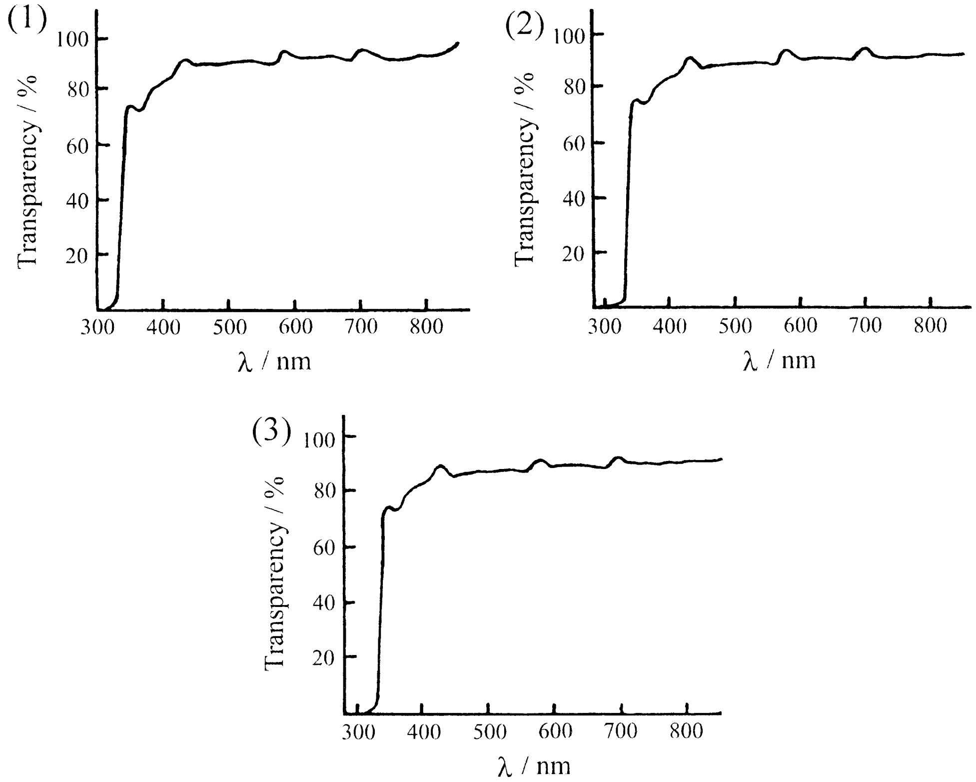

Fig. 6. The transparency of the ceramic inks. (1) Triton X-100/*n*-hexanol/cyclohexane/water reverse microemulsion; (2) ink; (3) ink B.

Zr^{4+}. The mixing of the two reverse microemulsions caused the formation of numerous $Zr(OH)_4$ precipitates, which destroyed the interface of oil–water to some degree, led to the reduction in transparency and the enhancement in viscosity. Therefore, the concentration of zirconium oxychloride solution and ammonia solution should be lowered a little to ensure satisfactory quality. According to this, two ceramic inks named A and B were prepared and listed in Table 5.

3.3. The physicochemical properties of ZrO_2 ceramic inks

3.3.1. Conductivity

When pH value of the ceramic inks was lower than 8, their conductivity did not change remarkably, remaining at 16–24 and 28–32 mS/m for inks A and B, respectively (see Fig. 3). It is obvious that this conductivity value is lower than that required for the continuous ink-jet printer. This is mainly because the oil phase is the

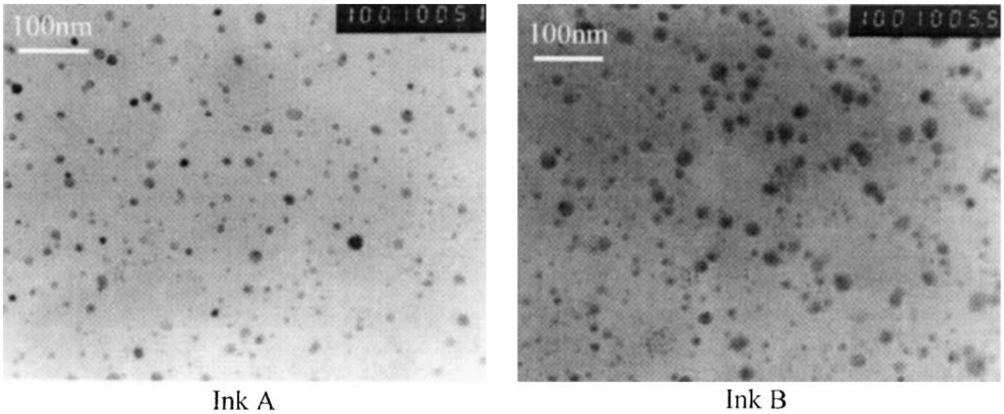

Fig. 7. The size and morphology of particles in the ceramic inks observed by TEM.

continuous one. These solutions exhibited a good state of RM. When the pH value exceeded 9, the RM was partly destroyed. Oil and water phases were mixed with each other, resulting in an increase in conductivity.

3.3.2. Surface tension

As shown in Fig. 4 the variation of surface tension was relatively small when the pH value of the ceramic inks changed. For ink A, it is only about 16–22 mN/m, lower than that required for the continuous printer. The surface tension of ceramic ink B lies in the range suitable to the printer's requirement in a wide range of pH value, but close to the lower limit. It is only 35 mN/m when the pH = 9.

3.3.3. Rheology

From the relation between viscosity and shear rate of the ceramic inks (Fig. 5), it is found that no effect of shear thickening was observed for ink A, but this effect occurred in a slight extent for ink B, which is no benefit to printing forming. It is seen that the viscosity of the inks A and B met the demand of the printer.

3.3.4. Transparency

The comparisons of transparency among the inks A and B and the pure system of Triton X-100/*n*-hexanol/cyclohexane/water reverse microemulsion were shown in Fig. 6. It can be obviously seen that the patterns of these spectra were basically identical except that the peak shifted backwards and transparency decreased a little with an increase in the concentration of the inks and increasing pH value. This demonstrated that inks A and B were very good reverse microemulsions. The inner structure of the three had nearly no difference.

3.3.5. TEM observation

Fig. 7 showed that the morphology and particle size of both inks were almost same. The particle size is about 7–10 nm. The photographs showed that these inks exhibited a very good dispersivity. No agglomerates were observed.

4. Conclusions

1. Triton X-100/*n*-hexanol/cyclohexane/water reverse microemulsion system was chosen and optimized from several other systems of reverse microemulsion to prepare ZrO_2 ceramic ink because it exhibited an excellent behavior in enhancing water-dissolving amount.
2. The best composition for the maximum water content of the above system was 19.1% Triton X-100/12.8% *n*-hexanol/23.7% cyclohexane/44.4% water in mass determined by its quasi-ternary phase diagram.
3. Two clear reverse microemulsions were obtained by replacement of the water in the system with equivalent volume of zirconium oxychloride solution and ammonia solution, respectively.
4. ZrO_2 ceramic inks prepared by reaction after mixing the two reverse microemulsions uniformly demonstrated excellent stability, dispersivity and homogeneity.
5. They were suitable for ink-jet printing forming by a drop on demand ink-jet printer through determinations of the physicochemical properties of the inks, such as viscosity, surface tension and transparency etc.
6. Their conductivity was not sufficiently high according to the requirements of the printer due to the continuous phase of oil.
7. The particle size in the reverse microemulsions was about 7–10 nm and very well dispersed by TEM observation.
8. It is still necessary to increase the solid load in the suspension further.

Acknowledgements

This paper was supported by National Natural Science Foundation of China under Grant No. 59972023.

References

1. Marcus, H. L., Beaman, J., Barlow, S. J. W. and Boumell, D. L., Solide freeform fabrication: powder processing. *Am. Ceram. Soc. Bull.*, 1990, **69**(6), 1030–1031.
2. Subramanian, P. K. and Marcus, H. L., Selective laser sintering of alumina using alumina binder. *Mater. Manuf. Processes*, 1995, **10**(4), 689–706.
3. Subramanian, P., *Selective Laser Sintering of Alumina*. PhD dissertaion. The University of Texas at Austin, 1995.
4. Klosterman, D., Chartoff, R., Graves, G. and Osborne, N. *et al.*, Direct fabrication of ceramics and composites through laminated object manufacturing (LOM). *International SAMPE Symposium and Exhibition (Proceedings)*, 1998, **43**(1), 693–705.
5. Klosterman, D. A., Chartoff, R. P. and Pak, S. S., Affordable rapid composite tooling via laminated object manufacturing. *International SAMPE Symposium and Exhibition (Proceedings)*, 1996, **41**(1), 220–229.
6. Griffin, C., Bautenbach, D. and McMillin, S., Desktop manufacturing: LOM vs pressing. *Am. Ceram. Soc. Bull.*, 1994, **73**(8), 80–113.
7. Danforth, S. C., Fused Deposition of Ceramics: a new technique for the rapid fabrication of ceramics components. *Mater. Technol.*, 1999, **10**(7–8), 144–146.
8. Agarwala, M. K., Jamalabad, V. R., Langrana, N. A., Safari, A., Whalen, P. J. and Danforth, S. C., Structural quality of parts processed by fused deposition. *Rapid Prototyping J.*, 1996, **2**, 4–19.
9. Agarwala, M. K., Bandyopadhyay, A., Weeren, R. V., Safari, A., Danforth, S. C., Langrana, N. A., Jamalabad, V. R. and Whalen, P. J., FDC, rapid fabrication of structural components. *Am. Ceram. Soc. Bull.*, 1996, **75**(11), 60–66.
10. Michali, W., Gemot, T., Krampe, E. and Langan, M., Stereolithography—a rapid prototyping method. *Kunststoffe*, 1994, **84**, 9–10.
11. Griffith, M. L. and Halloran, J. W., Stereolithography of ceramics. *Int. SAMPE tech. Conf*, 1995, **27**, 970–979.
12. Griffith, M. L. and Halloran, J. W., Freeform fabrication of ceramics via stereolithography. *J. Am. Ceram. Soc.*, 1996, **79**(10), 2601–2608.
13. Sachs, E., Cima, M., Williams, P., Brancazio, D. and Cornie, J., Three dimensional printing, rapid tooling and prototypes directly from a CAD model. *J. Eng. For Industry-Transactions of the AMSE*, 1992, **114**(4), 481–488.
14. Yoo, J., Cima, M., Sachs, E. and Suresh, S., Fabrication and microstructural control of advanced ceramics components by three dimensional printing. *Ceram. Eng. Sci. Proc*, 1995, **16**(5), 755–762.
15. Grau, J., Cima, M. and Sachs, E., Fabricating alumina molds for slip casting and 3-D printing. *Ceram. Ind.*, 1996, **146**(7), 22–27.
16. Teng, W. D. and Edirsinghe, M. J., Development of continuous direct ink-jet printing of ceramics. *Br. Ceram. Trans.*, 1998, **97**(4), 169–173.
17. Xiang, Q. F., Evans, J. R. G., Edirisinghe, M. J. and Blazdell, P. F., Solid freeforming of ceramics using a drop-on-demand jet printer. *Proc. Inst Mech. Eng., Part B*, 1997, **211**(B3), 211–214.
18. Ma, S.H., Matrick, H., Shor, A.C., Spinelli, H.J., Shepard, M.E., Hochberg, J., Aqueous pigmented ink for ink jet printers, US Patent 5221334, 1993, June.
19. Mott, M, Song, J.-H. and Evans, J. R. G., Microengineering of ceramics by direct ink-jet printing. *J. Am. Ceram. Soc.*, 1999, **82**(7), 1653–1658.
20. Blazdell, P. F., Evans, J. R. G., Edirisinghe, M. J., Shaw, P. and Binstead, M. J., Computer aided manufacture of ceramics using multilayer jet printing. *J. Mater. Sci. Lett.*, 1999, **14**(22), 1562–1568.
21. Teng, W. D. and Edirisinghe, M. J., Development of ceramic inks for jet printing: effect of conductivity. *Key Eng. Mater.*, 1997, **132–136**, 337–340.
22. Song, J. H., Edirisinghe, M. J. and Evans, J. R. G., Formulation and multilayer jet printing of ceramic inks. *J. Am. Ceram. Soc.*, 1999, **82**(12), 3374–3380.
23. Teng, W. D., Edirisinghe, M. J. and Evans, J. R. G., Optimization of dispersion and viscosity of a ceramic jet printing ink. *J. Am. Ceram. Soc.*, 1997, **80**(2), 486–494.
24. Ding, X., *Study on the Free-forming of Ink-jet Printing of Ceramic Inks*. PhD dissertation, Tianjin University. *Tianjin, 2001.*
25. Wang, R., *Research on Ceramic Ink for Computer Aided Ink Jet Printing Freeform*. Master Degree Dissertation, Tianjin University. *Tianjin, 1999.*
26. Briuker, C J., *Sol-Gel Science*. Academic Press, Inc, 1990.
27. Yang, S., *Research on Preparation of Ceramic Inks by Sol-gel Technique*. Bachelor Degree Dissertation, Tianjin University. *Tianjin, 2000.*
28. Guo, R., Qi, H., Guo, D., Lv, X. and Chen, Y., Preparation methods of ceramic inks for jet-printing forming. *J. Inorganic Materials*, 2001, **16**(6), 1049–1054.
29. Guo, R., Ding, X., Liang, Q., Guo, D., Qi, H., Yang, Z. and Chen, Y., Preparation and parameters of ZrO_2 ceramic ink for jet-printing forming. *Chinese J. Materials Research*, 2001, **15**(5), 583–586.
30. Guo, R., Qi, H., Chen, X., Yang, Z., Chen, Y., Preparation of high concentration ceramic ink for jet-printing forming (I). *J. Chinese Ceram. Soc.* (submitted for publication).
31. Guo, R., Qi, H., Chen, X., Yang, Z., Chen, Y., Preparation of high concentration ZrO_2 ceramic ink for jet-printing forming (II). Submitted to *J. Chinese Ceram. Soc.* (submitted for publication).
32. Li, X., Lin, E., Zhao, G. and Xiao, T., Microemulsion formation and phase behavior of anionic and cationic surfactants with sodium dodecyl sulfate and cetyltrimethylammonium bromide. *J. Coll. And. Inter. Sci.*, 1996, **184**(1), 20–30.
33. Anuradha, T. V. and Ranganathan, S., Synthesis of mesoporous materials based on titanium (IV) oxide and titanium nitride. *Nanostructured Materials*, 1999, **12**(5), 1063–1069.
34. Jafelicci Jr., M., Davolos, M. R., dos Santos, F. J. and de Andrade, S. J., Hollow silica particles from microemulsion. *J. Non-Crystalline Solids*, 1999, **247**, 98–102.
35. Chive, A. D., Bruno, B. and Maurice, B., Mechanism of formation of colloidal particles of calcium thiophosphates in an organic medium. *Langmuir*, 1998, **14**(19), 5355–5365.
36. Sangregorio, C., Carpenter, E.E., O'Connor, C.J., Synthesis and characterization of antiferromagnetic $KMnF_3$ nanoparticles, In *Materials Research Society Symposium—Proceedings 577*, Materials Research Society, 1999, p.435–441.
37. Arriagada, F. J. and Osseo-Asare, K., Synthesis of nanosize silica in aerosol OT reverse microemulsions. *J. Colloid Interface Sci.*, 1995, **170**(1), 8–17.
38. Ma, J., Huang, X., Cheng, H., Zhao, Z. and Qi, L., Preparation of nanosized ZnS particles in water/oil emulsions by microwave heating. *J. Mater. Sci. Lett.*, 1996, **15**(14), 1247–1248.

39. Motte, L., Billoudet, F. and Pileni, M. P., Synthesis in situ of nanosize silver sulphide semiconductor particles in reverse micelles. *J. Mater. Sci.*, 1996, **31**(1), 38–42.
40. Suzuki, K., Mizutani, N. and Harada, M., Preparation of cadmium sulfide ultrafine particles in various states with aid of cadmium dioleylphosphate microemulsion. *J. Chem. Eng. Japan*, 1999, **32**(5), 588–593.
41. Lee, M. H., Oh, S. G., Yi, S. C., Seo, D. S., Hong, J. P., Kim, C. O., Yoo, Y. K. and Yoo, J. S., Characterization of Eu-doped Y_2O_3 nanoparticles prepared in nonionic reverse microemulsions in relation to their application for field emission display. *J. Electrochem. Soc.*, 2000, **147**(8), 3139–3142.
42. Qi, L., Ma, J., Cheng, H. and Zhao, Z., Preparation of $BaSO_4$ nanoparticles in non-ionic w/o microemulsions. *Colloids and Surfaces A: Physicochemical and Engineering Aspects*, 1996, **108**(1), 117–126.